Some Microphysical Properties of an Ice Cloud from Lidar Observation of Horizontally Oriented Crystals

C. M. R. PLATT[1]

Cooperative Institute for Research in Environmental Sciences, University of Colorado/NOAA, Boulder 80309

N. L. ABSHIRE AND G. T. MCNICE

Wave Propagation Laboratory, NOAA, Boulder 80302

(Manuscript received 28 November 1977, in final form 7 April 1978)

ABSTRACT

Lidar observations of a winter ice cloud in the zenith gave a very high reflection but a very small depolarization. When the lidar was tilted more than 0.5° away from the zenith, the reflection amplitude fell to 3% of it's zenith value, but the depolarization increased. The above properties proved unambiguously that reflection was occurring from the specular surfaces of horizontal crystals. These properties were used to estimate some cloud microphysical properties. At a selected time, the estimates gave a mean "diameter" of 74 μm for the horizontal faces, a crystal number density of 0.78 ℓ^{-1}, and a maximum departure of the crystal axis from the horizontal of 0.5°. The fraction of the total crystal cross section which was specularly reflecting was estimated as unity.

1. Introduction

The depolarization ratio obtained from a linear polarized lidar pulse when reflected from a population of cloud particles has been shown to give a measure of cloud glaciation (Schotland *et al.*, 1971; Sassen, 1974) and possibly some information on cloud crystal habit (Sassen, 1977). Recently, Platt (1977) reported some very high-amplitude lidar reflections from a middle-level cloud when observed in the vertical, and an attendant low depolarization. Subsequently, these results were interpreted in terms of reflections from horizontally aligned hexagonal plate crystals (Platt, 1978; hereafter referred to as Pl). In Pl the backscatter properties of large, horizontally aligned plate crystals were analyzed. It was shown that information on the crystal number density, size and the quality of the crystals could be estimated provided that the change in the magnitude of the backscatter coefficient with angle near the zenith and the depolarization ratio were measured. In previous measurements (Platt, 1977), the lidar was not scanned away from the vertical, but the backscatter coefficients and depolarization ratios for vertical viewing were consistent with the above interpretation. It was apparent that reflections were occurring specularly from a few crystals in each pulse volume which happened to be correctly aligned. This would explain, quite simply, the low depolarization (Liou and Lahore, 1974; Chýlek, 1977) and high backscatter.

[1] On leave from CSIRO, Division of Atmospheric Physics, Aspendale, Victoria, 3195, Australia.

Subsequent to the work in Pl, lidar observations were made on a winter ice cloud near Boulder, CO. When the lidar was scanned away from the vertical a dramatic decrease in lidar backscatter occurred. For a zenith angle of only 0.5° the backscatter decreased to about 3% of the zenith value. This fact, together with the high backscatter coefficients and low depolarization ratios observed in the zenith were strong evidence that the lidar was observing specular reflections from ice crystal plates with their long axes aligned in the horizontal. For if the lidar scan was at a zenith angle which was greater than the maximum angle of departure of the crystal long axes from the horizontal (the flutter angle) then all specularly reflected light would be directed away from the lidar receiver, and the receiver signal would indeed drop dramatically. For greater zenith angles the signal would be composed of light which had undergone multiple internal reflections within the crystals.

In this note the observations made near Boulder are described, together with estimates of the maximum angle of flutter of the crystals and their number densities and sizes.

2. Lidar and aircraft measurements

The lidar measurements were made with the WPL/ERL/NOAA monostatic lidar (Derr *et al.*, 1976), at a site about 8 mi north of Boulder. The lidar was pointed in the vertical and then scanned away from the vertical in small-angle increments. Calibrated values of the backscatter coefficient and the depolariza-

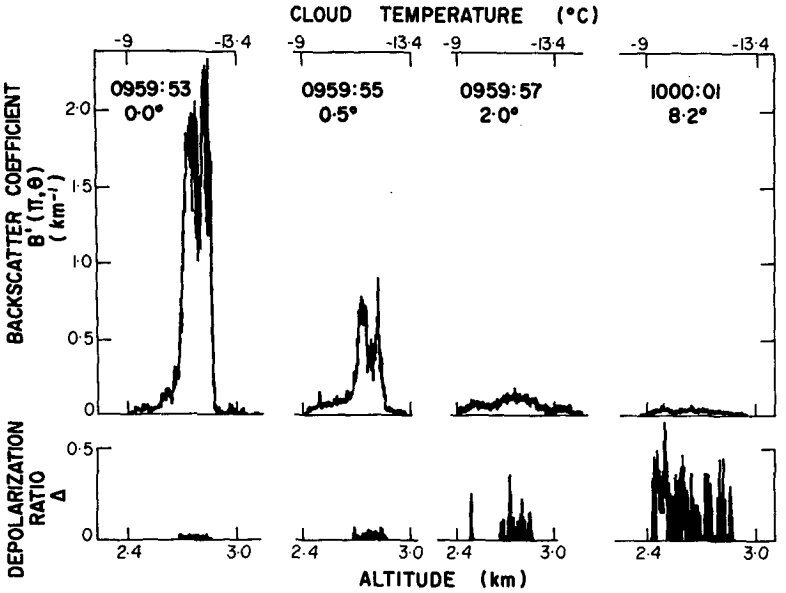

FIG. 1. Cloud backscatter coefficients $B'(\pi,\theta)$ and depolarization ratios for zenith angles of (a) 0.0°, (b) 0.5°, (c) 2.0° and (d) 8.2° at the times shown.

tion ratio and their variations with range were recorded for each angle. The scans were repeated at regular intervals.

An instrumented aircraft obtained simultaneous measurements of temperature versus altitude. Visual pilot observations indicated an ice cloud. A strong subsun was observed below the aircraft when flying in, or above, the cloud, which gave independent evidence of the presence of oriented crystals.

The cloud was observed on 24 January 1977. It was rather tenuous in nature and the ground was visible to the pilot through the cloud for most of the time.

A series of lidar returns are shown in Fig. 1. It is obvious, immediately, that the cloud returns have the characteristic features predicted for horizontal ice crystals. The reduction in backscatter for 0.5° zenith angle is quite large. For $\theta=2.0°$ the backscatter is an order of magnitude smaller. The depolarization ratio is seen to vary from about 0.01 at $\theta=0.0°$ to values in the region of 0.3 at $\theta=8.2°$. Two further cloud profiles taken in the vertical are shown in Figs. 2 and 3. The backscatter coefficient $B(\pi)$ is very high and the depolarization ratio is almost vanishingly small. These profiles were among the strongest recorded and are discussed later.

3. Discussion

Several lidar scans away from the vertical were made during the observation period, with the lidar being fired at small-angle increments. A convenient method of obtaining the relative intensity of backscatter at each zenith angle θ is to calculate $\gamma'(\pi,\theta)$, the integrated backscatter through the cloud,

$$\gamma'(\pi,\theta)=\int_{z_b}^{z_T} B'(\pi,\theta)dz, \tag{1}$$

where it is understood that $B'(\pi,\theta)$ is the measured isotropic backscatter coefficient at angle θ and z_b and z_T are the cloud base and top, respectively. Attenuation of the pulse in the cloud causes $B'(\pi,\theta)$ to be less than its actual value $B(\pi,\theta)$. However, in this cloud there was evidence that attenuation was very low. First, pilot reports indicated a tenuous cloud, with the ground usually visible through the cloud. Second, the very high backscatter in Fig. 3 shows very little apparent attenuation toward cloud top, and the attenuation would be even smaller for the other cases with lower backscatter. The intensity $\gamma'(\pi,0)$ can be compared with $\gamma'(\pi,\theta)$ at zenith angle θ to estimate the maximum angle of crystal flutter $\delta\xi$. The ratio of $\gamma'(\pi,\theta)$ to $\gamma'(\pi,0)$ for angles near and at the zenith and for four separate lidar scans between 0930 and 1030 LT are shown in Fig. 4. A line of best fit was drawn by eye through unity ratio at zero zenith angle and the four other points. The horizontal broken line shows the typical value of $\gamma'(\pi,\theta)/\gamma'(\pi,0)$ found for angles $\geqslant 0.6°$. The value of θ at the intersection of the lines is defined here as the maximum angle of flutter $\delta\xi$. This definition gives $\delta\xi=0.56°$. However, 0.06° must be subtracted for the transmitter beamwidth, so that $\delta\xi\approx 0.5°$.

The number of crystals in the lidar pulse volume which are correctly aligned for specular reflection to the receiver is very sensitive to the maximum angle of crystal flutter, $\delta\xi$, assuming that the crystals' axes have two degrees of freedom of rotation about the horizontal. Signal "spikes" which are probably due

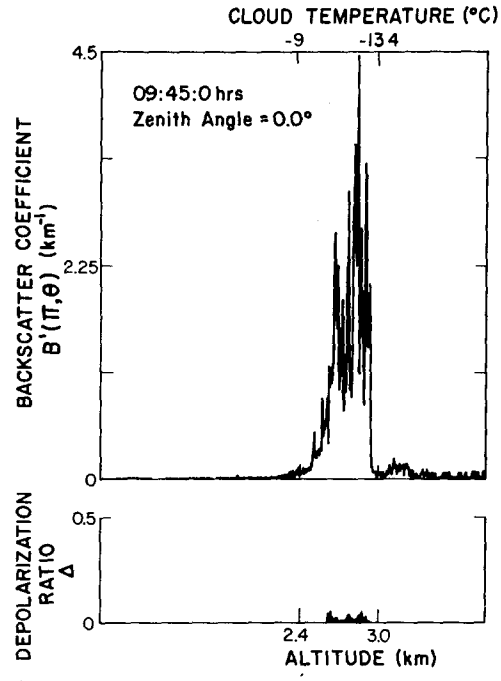

FIG. 2. Cloud backscatter coefficients and depolarization ratio profiles when the cloud was fairly homogeneous and showing single crystal "spikes."

to reflections from a single crystal are evident in the profiles of Figs. 1 (0.5°) and 2, near the cloud base. For a given lidar geometry, the backscatter coefficient of one "spike" will give a measure of the area of specular reflection from an individual crystal.

Toward the cloud centers, the large and fluctuating signal indicates that more than one reflection is being obtained in each pulse volume. An estimation of the average number in each volume can be made, leading to a cloud number density. Finally, for the cases of many reflections from each pulse volume, the average signal together with the estimated crystal diameters and angle of flutter, will give an estimate of the *fraction* of the total crystal cross-section which is specularly reflecting. The above aspects are considered separately below to give a tentative picture of the cloud microphysics at one time (Fig. 2).

The power returned to the receiver from a single crystal is given in Pl as

$$P_R = P_0(2RA/z^2\delta\phi)[\exp(-2\tau_{atm})], \qquad (2)$$

where P_0 is the transmitter power, A the crystal reflecting cross-section, z the range, $\delta\phi$ the solid angle of the transmitter beam, R the normal reflectivity of the crystal surface, and τ_{atm} the atmospheric optical depth at the laser wavelength between the cloud and the ground.

In terms of the backscatter coefficient $B(\pi)$, the return power is given by the standard lidar equation

$$P_R = P_0[c\Delta t A_1 B(\pi)/8\pi z^2] \exp(-2\tau_{atm}), \qquad (3)$$

where c is the velocity of light, Δt the pulse duration and A_1 the receiver aperture. Combining Eqs. (2) and (3) will give the individual crystal area for a given measured maximum backscatter coefficient of the "spike" signal

$$A = (c\Delta t A_1 \delta\phi/16\pi R)B(\pi). \qquad (4)$$

Values of A_1 and Δt for the NOAA lidar are shown in Table 1. Using these figures and $R=0.02$ (Pl) we obtain a value for A of 1.08×10^{-8} m^2 per unity backscatter coefficient (in km^{-1}). For simple hexagonal crystals we assume that the cross section is circular and thus a crystal radius can be defined. This radius is given for the NOAA lidar by

$$r = 59\sqrt{B(\pi)}\ \mu\text{m}, \qquad (5)$$

where $B(\pi)$ is now in units per kilometer. In many cases, the spike signals in the pulse volume overlap. However, if we assume that the number of spike signals arising from a pulse volume is given by a statistical distribution about a mean value and we also ignore the small contribution to the signal by non-aligned crystals, then the mean backscatter coefficient will give a measure of the product of the number n of crystals and their backscatter coefficients $B(\pi)$. Further, the "noise" fluctuation level through the cloud (assuming a homogeneous cloud) compared to the mean signal will be related to n. Thus, assuming Poisson statistics, $n=(\text{SN})^2$, where SN is the mean signal-to-noise ratio. It is apparent from many of the returns, i.e., Fig. 1 (0.5°) and Fig. 3 that the cloud is not homogeneous with altitude.

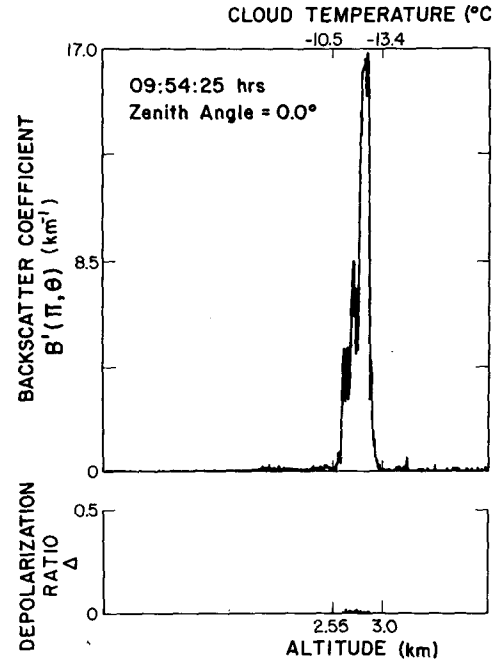

FIG. 3. Very high cloud backscatter coefficients and very low depolarization ratios. The angle of flutter may have decreased.

Also, the noise on the very weak signals at $\theta=2°$ and 8.2° in Fig. 1 is photon and instrumental noise rather than noise from signal spikes. However, Fig. 2 shows more uniform "noise" and at a level which is much greater than photon noise. The mean backscatter coefficient, defined here as $\gamma'(\pi)/h$, where h is the cloud depth, is ~ 2 km^{-1}. The rms "spike" noise is estimated by eye to be 0.9 km^{-1}. Thus, SN$\approx$2.2, from which $n\approx 4.8$. This indicates that each spike signal has a backscatter coefficient of 0.4 km^{-1}, on average. From Eq. (4), the radius of the crystal is 37 μm. The small spikes near the cloud base have a $B(\pi)$ of about 0.25 km^{-1}, yielding a crystal radius of 29 μm.

The number of crystals n_a optimally aligned in a lidar pulse volume is given in Pl as

$$n_a=\pi n_0 l D^2(\delta\theta/8\delta\xi)^2, \tag{6}$$

where $\delta\theta$ is the transmitter beam angle ($<\delta\xi$), n_0 the crystal number density, l the pulse length and D the receiver diameter. The fundamental assumption in the derivation of this equation is that the main crystal axis is equally likely to take up any angle between horizontal and the angle $\delta\xi$ from the horizontal. Having obtained n_a, we can solve for n_0. For the lidar parameters of Table 1 and using $\delta\xi=0.5°$, $n_a=4.8$, (Fig. 2) we obtain $n_0\approx 0.8$ crystals l^{-1}.

Expressions for mean values of $B(\pi)_{\parallel}$ and $B(\pi)_{\perp}$ for the case where there are many overlapping spike signals in each pulse volume were also derived in Pl. $B(\pi)_{\parallel}$ and $B(\pi)_{\perp}$ are backscatter coefficients for radiation returned in the same polarization plane as the transmitter beam and in the orthogonal plane respectively. [Also, $B(\pi)=B(\pi)_{\parallel}+B(\pi)_{\perp}$.] The model assumes a mixture of anisotropic imperfect crystals for which $B(\pi)_{\parallel}=B(\pi)_{\perp}$ and perfectly reflecting crystals for which $B(\pi)_{\perp}=0$:

$$\left.\begin{aligned} B(\pi)_{\parallel}&=(n_0\pi d^2)[0.01f/(\delta\xi(1+2R))+0.25(1-f)]\\ B(\pi)_{\perp}&=(n_0\pi d^2/4)(0.25(1-f)) \end{aligned}\right\}, \tag{7}$$

where d is the crystal diameter and f the fraction of the total number of crystals which are specularly reflecting. Using $B(\pi)=2$ km^{-1}, $n_0=0.8^{-1}$, $d=74$ μm, we obtain $f\approx 1.0$. That the value of f equals unity is completely fortuitous. However, it might indicate that the crystals in the cloud were mostly well-formed hexagonal crystals. The temperature range in the cloud was from about -9 to -13°C, a range in which hexagonal crystals form, but without dendritic growth. Thus, it could be expected that many of the crystals would be perfectly formed. Finally, we consider Fig. 3. The mean backscatter coefficient is 7 km^{-1} and for the top part of the cloud it increases to 16 km^{-1}. The mean value is 3.5 times that in Fig. 2. If this increase was due to a growth in crystal *size* then *both* signal and noise would increase by 3.5, and the SN would still be 2.2. In fact just the opposite appears to have occurred and SN$\approx$7, so that $n_a\approx 49$. However, it is also possible that the maximum angle of flutter was less at 0954 than it had been at 0945. This would have the apparent effect of increasing both n_a and SN. The flutter angle was not measured at the time that Fig. 4 was obtained.

TABLE 1. WPL/ERL/NOAA lidar characteristics.

Transmitter	
Type	Pulsed ruby laser
Energy	2 J
Pulse length	30 ns
Beam divergence	1 mrad
Receiver	
Type	Newtonian
Area	1.54 m^2
Field of view	3 mrad
Polarizer	Polaroid
Electronic time-gate	60 ns

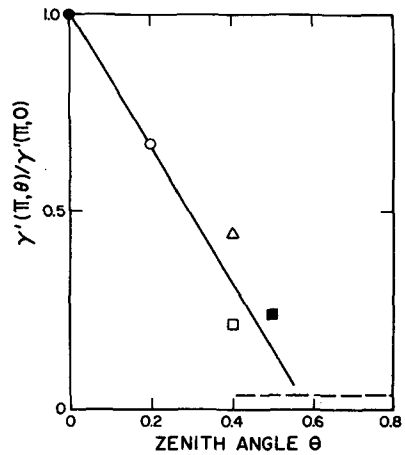

FIG. 4. The dependence of the integrated backscatter on the zenith angle, normalized to unity at $\theta=0.0$.

In summary, we can estimate the cloud properties of Fig. 2 as follows:

Cloud-base altitude $=2.4$ km
Cloud-top altitude $=3.0$ km
Temperature range $=-9$ to -13°C
Number density $=0.8\ l^{-1}$
Mean crystal diameter $=74$ μm
Average backscatter coefficient $=2$ km^{-1}
Maximum angle of departure of long axis of crystal from horizontal $=0.5°$
Fraction of total crystal cross section which is specularly reflecting ~ 1

The cloud at the time of Fig. 3 (9 min later) would be expected to have the same properties, except that n_0 has increased to $\sim 8\ l^{-1}$.

4. Conclusion

The angular properties of the lidar backscatter from the observed cloud prove rather conclusively that ice crystals with their large axes oriented in the horizontal were being observed. These properties are similar to those predicted in Pl. Although the calculations presented here are necessarily very tentative, they indicate the type of information on the cloud microstructure which might be obtained. By tailoring the lidar geometry (e.g., using a very narrow transmitting beam), single crystal reflections from a pulse volume could be observed, and their radii could be deduced.

Signal "spikes" were first noted by Schotland *et al.* (1971) in a laboratory experiment. They concluded also that the signals originated from reflections off crystal planar surfaces. Sassen (1977) subsequently demonstrated that the crystal diameters calculated from spike signals compared favorably with the diameters measured directly. Sassen used a continuous laser which measured the spike amplitudes and numbers as the crystals traveled through the laser beam. The lidar pulse method selects a volume of cloud and measures the number of spikes and their amplitudes at one single time.

The large backscatter coefficients of Figs. 1–3 are further evidence that specular reflections are being observed. The calculated value of $\gamma'(\pi)$ in Fig. 3 was 2.78, which is much greater than that measured for cirrus clouds (Platt, 1973) and compares with the value of 7.6 obtained by Platt (1977a) from an altostratus cloud layer. For that cloud it was also suspected that the layer might be composed of horizontally oriented crystals as the depolarization was also low but no scans away from the vertical were made.

The presence of preferred orientation in ice crystal clouds has, of course, been known for many years from the large variety of optical effects obtained when the clouds are illuminated by the sun. However, it is apparent that lidar measurements can give more definitive information on crystal orientation and on the cloud microstructure.

Acknowledgments. One of the authors (C. M. R. Platt) is indebted to CIRES for a Visiting Fellowship, to Dr. V. E. Derr and his atmospheric spectroscopy group for the use of data taken with the NOAA lidar, for the excellent data reduction facilities and for much help and encouragement.

REFERENCES

Chýlek, P., 1977: Depolarization of electromagnetic radiation scattered by non-spherical particles. *J. Opt. Soc. Amer.*, **67**, 175–178.

Derr, V. E., N. L. Abshire, R. E. Cupp and G. T. McNice, 1976: Depolarization of lidar reforms from virga and source cloud. *J. Appl. Meteor.*, **15**, 1200–1203.

Liou, Kuo-Nan, and H. Lahore, 1974: Laser sensing of cloud composition: A backscattered depolarization technique. *J. Appl. Meteor.*, **13**, 257–263.

Platt, C. M. R., 1973: Lidar and radiometer observations of cirrus clouds. *J. Atmos. Sci.*, **30**, 1191–1204.

——, 1977: Lidar observation of a mixed-phase altostratus cloud. *J. Appl. Meteor.*, **16**, 339–345.

——, 1978: Lidar backscatter from horizontal ice crystal plates. *J. Appl. Meteor.*, **17**, 482–488.

Sassen, K., 1974: Depolarization of laser light backscattered by artificial clouds. *J. Appl. Meteor.*, **13**, 923–933.

——, 1977: Ice Crystal habit discrimination with the optical backscatter depolarization technique. *J. Appl. Meteor.*, **16**, 425–431.

Schotland, R. M., K. Sassen and R. Stone, 1971: Observations by l idar of linear depolarization ratios for hydrometers. *J. Appl. Meteor.*, **10**, 1011–1017.